EPJ Web of Conferences will be set by the publisher
DOI: will be set by the publisher
© Owned by the authors, published by EDP Sciences, 2015

Status of the Mu3e Experiment at PSI

Ann-Kathrin Perrevoort[1,a] for the Mu3e Collaboration

[1] *Physikalisches Institut, Heidelberg University, Im Neuenheimer Feld 226, 69120 Heidelberg, Germany*

Abstract. The Mu3e experiment aims to search for the lepton-flavour violating decay $\mu^+ \to e^+e^+e^-$ with a sensitivity to one signal decay in 10^{16} muon decays at a muon stopping rate of 2×10^9 muons/s. With currently available rates of 10^8 muons/s, a sensitivity on the branching ratio of 10^{-15} is aimed at in a first phase. This would allow to test new physics models with enhanced branching ratios for lepton-flavour violating processes with unprecedented precision.
The experiment has to be operated at very high muon rates while background of the decay $\mu^+ \to e^+e^-e^+\overline{\nu}_\mu\nu_e$ and accidental combinations of positrons and electrons has to be suppressed below sensitivity level. Therefore, a tracking detector made of thin pixel sensors with additional scintillating fibres and tiles for precise time measurement will be built. Currently, development of the subdetectors is ongoing while detector construction is in preparation.

1 Introduction

The Mu3e experiment is dedicated to search for physics beyond the Standard Model (BSM) via the lepton flavour-violating decay $\mu^+ \to e^+e^+e^-$.
In principle, this process can be mediated via neutrino mixing, see Fig. 1(a), but as it is suppressed to a branching ratio below 10^{-54}, any observation would be a clear sign for new physics. And in fact, many BSM models naturally predict enhanced branching ratios for charged lepton flavour violating processes like $\mu \to eee$ [1].
In BSM models, the $\mu \to eee$ decay can be mediated at lowest order by dipole-like interactions (see Fig. 1(b)) or four-fermion contact interactions (see Fig. 1(c)) depending on the particular model.
In [2], the $\mu \to eee$ and $\mu \to e\gamma$ decay have been studied by the means of effective field theory. Depending on the underlying interaction, a search for $\mu \to eee$ with a sensitivity of 10^{-16} on the branching ratio is able to test the effective mass scale of lepton-flavour violating operators in the range of several thousand TeV (see Fig. 2).
The current limit on the process $\mu \to eee$ has been set by the SINDRUM experiment to $BR_{\mu\to eee} < 1.0 \times 10^{-12}$ at 90 % confidence level (CL) [3]. The Mu3e experiment aims to search for $\mu \to eee$ with a sensitivity on the branching ratio of 10^{-15} at 90 % CL in the first stage of the experiment, and 10^{-16} at 90 % CL in the second stage [4].

2 Signal and Background

Experimentally, the $\mu^+ \to e^+e^+e^-$ decay is identified by measuring two positrons and an electron from a common vertex in space and time. As in the Mu3e experiment the antimuons decay at rest, the energies of the electron and positrons sum up to the muon mass, whereas the sum of their momenta vanishes. Any other process that mimics this signature is a potential source of background and needs to be suppressed in the experiment to below the sensitivity level.
One source of background is accidental combinations of any two positrons and an electron that, within the detector resolution, show the characteristics of the signal decay – e.g. a positron from the dominant Michel decay $\mu^+ \to e^+\overline{\nu}_\mu\nu_e$ in combination with a positron and electron from a Bhabha scattering event or photon conversion. The higher the rate of incoming antimuons is, the more likely are accidental combinations. This source of background can be controlled by good time, vertex and momentum resolution.
Furthermore, the radiative decay of the antimuon with internal conversion $\mu^+ \to e^+e^-e^+\overline{\nu}_\mu\nu_e$ has a similar signature as the signal decay. The undetected neutrinos create missing energy, thus an excellent momentum resolution is crucial in order to control this type of background. This is illustrated by Fig. 3 which shows the integrated branching ratio for the internal conversion decay for different cut values on the sum of the energies of the three decay particles E_{tot}.
A momentum resolution of about 0.5 MeV turns out to be necessary to sufficiently suppress internal conversion decays. This is particularly challenging to achieve as the electrons[1] have a low momentum and thus are strongly affected by multiple Coulomb scattering which in turn af-

[a] e-mail: perrevoort@physi.uni-heidelberg.de

[1] Here and in the following, electrons and positrons will simply be denoted as electrons. In the same way, muons and antimuons will be referred to as muons.

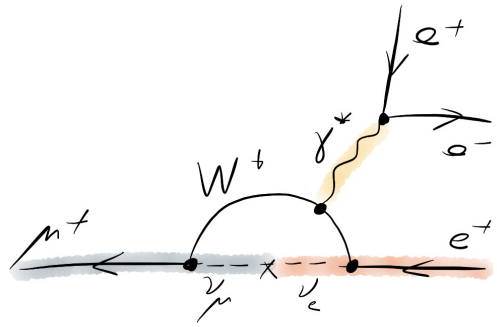

(a) The decay μ → eee mediated by neutrino mixing in the Standard Model.

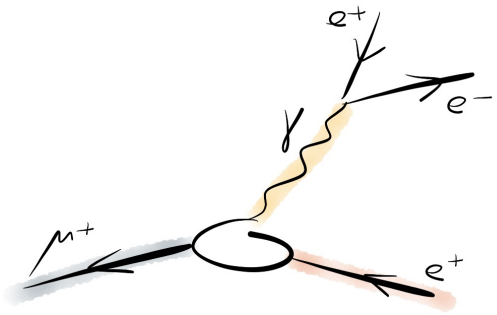

(b) The μ → eee decay at loop level in BSM models.

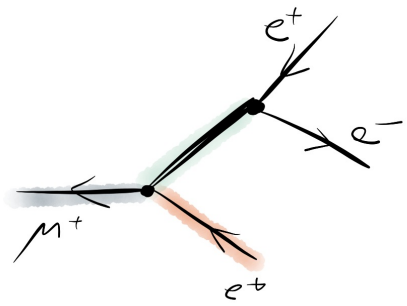

(c) The μ → eee decay at tree level in BSM models.

Figure 1. Diagrams of the decay μ → eee (a) mediated in the Standard Model via neutrino oscillations, and at (b) loop and (c) tree level in BSM models.

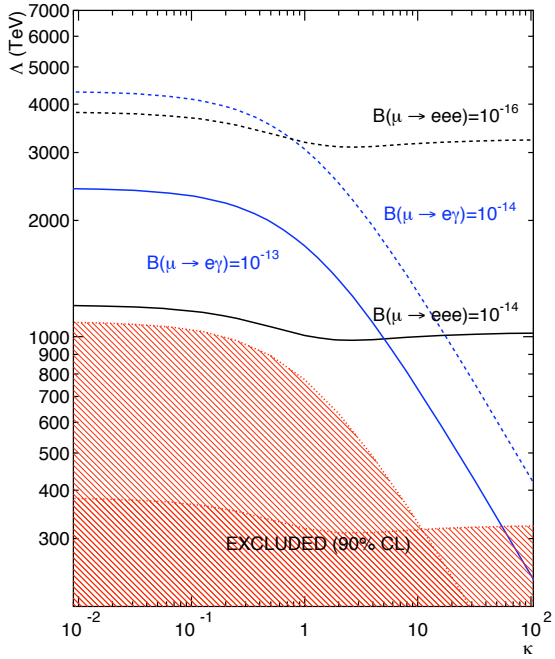

Figure 2. Comparison of the reach in effective mass scale Λ of new physics in searches for the decay μ → eγ and μ → eee. Low values of κ represent dominating dipole, high κ dominating four-fermion contact interactions. Taken from [2].

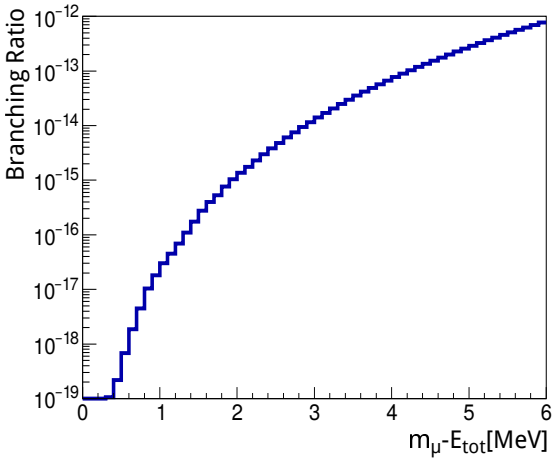

Figure 3. Integrated branching ratio for the radiative muon decay with internal conversion μ → eeeνν̄ for different cut values on the total energy E_{tot} of the three decay electrons. Adapted from [5], matrix element by [6].

fects the momentum measurement.
In addition, for the Mu3e experiment a vertex resolution of about 200 μm and a time resolution of ∼ 100 ps is envisaged.

3 Experimental Concept

The detector in the Mu3e experiment has to be able to cope with high muon stopping rates while the amount of material in the active detector volume has to be kept to a minimum. With thin pixel sensors, a high momentum resolution will be achieved, while scintillating fibres and tiles will allow for precise time measurements.
The Mu3e detector will be built in stages corresponding to an increase in the muon stopping rate.

3.1 Muon Beam

At the Paul-Scherrer Institute (PSI) a proton beam with 590 MeV is provided with a very high intensity of 2.2 mA. Pions and subsequently muons are produced on carbon tar-

gets. The πE5 beam line, currently used by the MEG experiment [7], is one of the most intense low energy muon beam lines at PSI. Here, rates of up to 10^8 muons/s of 28 MeV/c muons are available. It is planned, that the beam time at πE5 will be shared between the MEG and Mu3e experiment.
The envisaged sensitivity of 10^{-16} on the branching ratio, however, can only be reached by muon rates of about 2×10^9 muons/s. This would require a new beam line – a possibility that is currently under investigation at PSI.

3.2 Detector Design

In the Mu3e experiment, the incoming 28 MeV/c muon beam will be stopped in a hollow double-cone shaped target made of Mylar®. The shape of the target is chosen such that the decay vertices will spread over a large area which helps in reducing background from accidental combinations. As the target and detectors will be placed in a solenoidal magnetic field of 1 T, the momentum of the decay electrons will be measured by determining the bending radius of their trajectories. The pixel detector will be arranged in a barrel-type geometry around the beam axis (see Fig. 4).
In the first phase of the experiment – phase IA – there will be a double-layer of pixel sensors surrounding the target, and one double-layer at larger radii (see the central detector part in Fig. 4). The detector will be about 36 cm long with a radius of about 18 cm. At this stage, the experiment will be operated at 2×10^7 muons/s. This allows to reach a sensitivity to $\mu \rightarrow eee$ of 10^{-13} to 10^{-14} depending on the run time.
In order to improve the momentum resolution, the electrons will be measured again after they curl back to the detector. The acceptance for re-curling tracks will be increased by installing so-called recurl-stations upstream and downstream of the central detector part in phase IB of the experiment. The recurl-stations will consist as well of a double-layer of pixel sensors and will have the same dimensions as the central station.
An operation at 1×10^8 muons/s will become feasible in phase IB by installing additional timing detectors: scintillating fibres in the central detector part, and scintillating tiles in the additional recurl-stations. Thus, accidental combinations will be efficiently suppressed. With this detector configuration, a sensitivity of up to 10^{-15} can be reached.
Given a new beam line, the Mu3e experiment will be operated in phase II studying 2×10^9 muons/s. For this phase, an additional pair of recurl-stations will be installed, one recurl-station upstream and one downstream of the existing detector in order to increase the acceptance for re-curling tracks. In this configuration, the Mu3e experiment can reach its target sensitivity of 10^{-16}.

3.3 Pixel Sensors

The tracking detector in the Mu3e experiment will be built from silicon pixel sensors as they provide the high granularity necessary at high muon stopping rates [8].

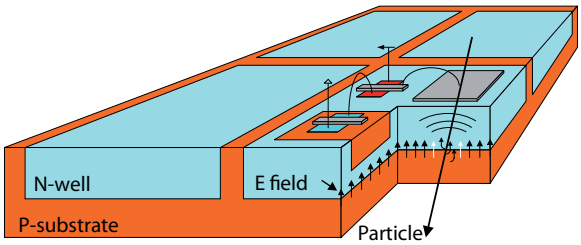

Figure 5. Schematic of a pixel sensor in HV-MAPS technology. Taken from [9].

The High-Voltage Monolithic Active Pixel Sensors (HV-MAPS) [9–13] technology has been chosen for the Mu3e experiment. The pixels are implemented as deep N-wells in a p-doped substrate, and are reversely biased by about 60 V to 90 V (see Fig. 5). Thus, charges generated by traversing particles are fastly collected via drift within $\mathcal{O}$(1 ns).
In addition, the charge collection is limited to a thin depleted zone close to the surface. Therefore, the sensors can be thinned to 50 µm which allows to build a very lightweight pixel detector.
Another advantage of the HV-MAPS is the possibility to implement analogue and digital logic directly on the sensor allowing for amplification and digitization of the signals already on the chip. No additional readout chip is needed as in standard hybrid pixel sensor designs.
In the experiment, HV-MAPS chips of a size of 2 cm×2 cm with a pixel size of 80 µm×80 µm and a thickness of 50 µm will be used.
The latest HV-MAPS prototype for the Mu3e experiment is the MuPix7. It is a small sensor with a size of 2.9 mm × 3.2 mm and a pixel size of 103 µm × 80 µm, but features already the full functionality of the final chip including an on-chip readout state machine. The output of the MuPix7 is zero-suppressed hit addresses and corresponding time stamps transmitted via a fast serial link at 1.25 Gbit/s.
The MuPix prototypes have been extensively tested in the laboratory and in testbeam campaigns [14, 15]. For MuPix7, efficiencies above 99 % for the entire test system at a noise rate of less than 100 Hz per pixel have been measured, as well as a time resolution of better than 12 ns. Thus, the requirements on the pixel sensor are met.

3.4 Lightweight Mechanics and Cooling

For the 50 µm thin pixel sensors 100 µm thick Kapton® based flexprints with aluminum or copper traces will be utilized to connect the signals to the front-end electronics and to power the sensors. In addition, the sensors with flexprints will be glued to a mechanical support structure built of 25 µm Kapton® foil. Thus, one layer of the pixel detector will contribute to the overall material budget with about 1 ‰ of a radiation length.
The sensors and electronics dissipate heat and need to be cooled. This will be done with gaseous helium. Helium is chosen as a coolant in order to minimize multiple Coulomb scattering in the detector volume.

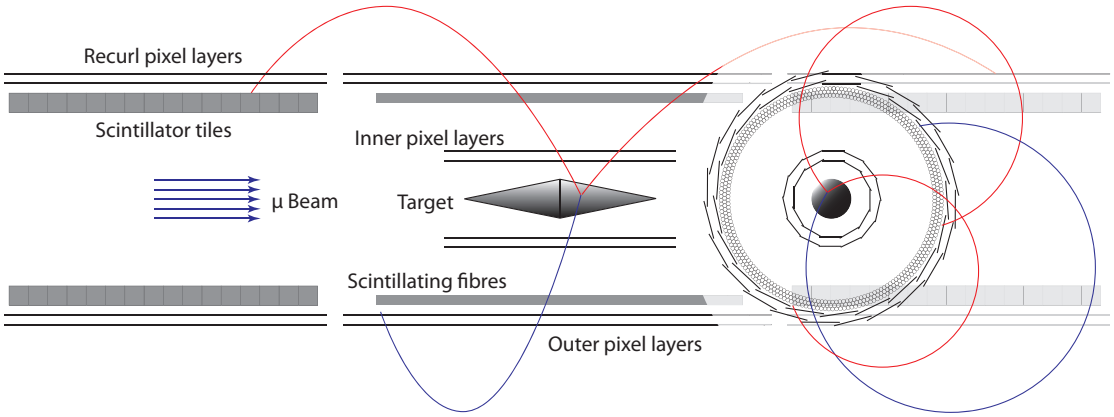

Figure 4. Schematic layout of the Mu3e detector in phase IB to be operated at 10^8 muons/s.

The cooling concept has been studied in simulation and is tested with mechanical prototypes built of Kapton® and thin glass plates [16].

3.5 Scintillating Fibres and Tiles

In order to improve the time resolution, the detector will be equipped with scintillating detectors from phase IB onward.
In the most central part, three layers of 250 µm thick scintillating fibres will be used that will be read out at both ends with silicon photo-multipliers (SiPMs). Fibres with round and squared cross section are currently under study. Current prototypes of scintillating fibre modules yield a time resolution of below 1 ns [17].
In the recurl-stations the amount of material is no longer an issue, and therefore scintillating tiles of about 0.2 cm^3 will be used. The tiles will also be read out by SiPMs. Current prototypes yield a time resolution of better than 100 ps [18].
The readout of the SiPMs of both fibres and tiles will be performed with a custom-designed ASIC, the so-called STiC chip [19, 20].

3.6 Data Acquisition

The final Mu3e detector will consist of nearly 300 million pixels and about 4000 scintillating fibres and 7000 scintillating tiles.
The data acquisition will be performed without a hardware trigger [21]. The sub-detectors will continuously send zero-suppressed data to the readout chain. At 2×10^9 muons/s, this will account for a data rate of about 1 Tbit/s. The data will then be forwarded to a filter farm consisting of PCs equipped with graphics processing units. On the filter farm, fast online track reconstruction will be performed and signal-like topologies are going to be looked for. Thus, the data rate written to mass storage will be reduced to less than 100 MB/s.

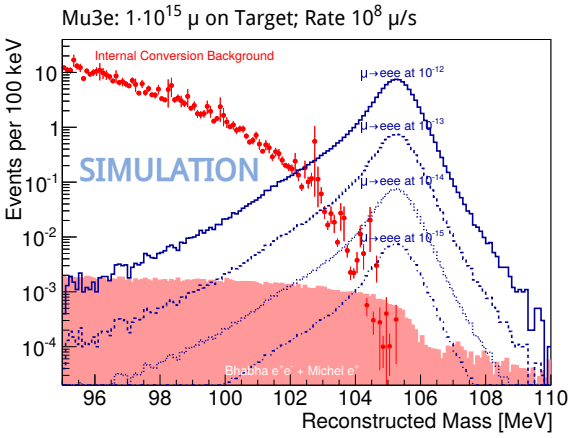

Figure 6. Reconstructed mass of three electrons from simulated internal conversion events, accidental combinations of Bhabha scattering events and Michel decays, and from the μ → eee signal decay at various branching ratios.

4 Sensitivity Studies

In order to estimate the detector performance, a full Geant4 [22, 23] based simulation of the Mu3e detector has been established.
The result for the phase IB detector configuration with 10^{15} muons on target at a rate of 10^8 muons/s can be seen in Fig. 6. It shows the reconstructed invariant mass of three electrons in the signal region from different sources of background, namely the radiative decay with internal conversion and accidental combinations of electrons from Bhabha scattering and the Michel decay, as well as signal events implemented as three body decays at different

branching ratios. The detector performs well enough to separate signal decays from background even at a branching ratio of 10^{-15}.

5 Status and Outlook

The research proposal [4] for the Mu3e experiment was approved at PSI in 2013. At the moment, the technical design report is being prepared and will be presented at PSI beginning of 2016.
Meanwhile, research and development on the subdetectors as well as the preparation of the detector construction is ongoing. Commissioning and first data-taking is expected for 2017.

A Acknowledgements

The author acknowledges support by the DFG Research Training Group on Particle Physics beyond the Standard Model.

References

[1] Y. Kuno, Y. Okada, Rev.Mod.Phys. **73**, 151-202 (2001)
[2] A. Gouvêa, P. Vogel, Prog.Part.Nucl.Phys. **71**, 75-92 (2013)
[3] U. Bellgardt et al., Nucl.Phys. **B299**, 1-6 (1988)
[4] A. Blondel et al., *Mu3e Research Proposal* (2013)
[5] R. Djilkibaev, R. Konoplich, Phys.Rev. **D79**, 073004 (2009)
[6] A. Signer et al., *private communication* (2015)
[7] J. Adam et al., Eur.Phys.J. **C73**, 2365 (2013)
[8] N. Berger et al., Nucl.Instrum.Meth. **A732**, 61-65 (2013)
[9] I. Perić, Nucl.Instrum.Meth. **A582**, 876-885 (2007)
[10] I. Perić, C. Takacs, Nucl.Instrum.Meth. **A624**, 504-508 (2010)
[11] I. Perić, C. Kreidl, P. Fischer, Nucl.Instrum.Meth. **A650**, 158-162 (2010)
[12] I. Perić et al., Nucl.Instrum.Meth. **A731**, 131-136 (2013)
[13] I. Perić et al., JINST **10**, C05021 (2015)
[14] S. Shrestha, PoS **TTIP2014**, 047 (2014)
[15] D. Wiedner et al., JINST **10**, C03044 (2015)
[16] D. Wiedner et al., JINST **9**, C08023 (2014)
[17] A. Bravar, Nucl.Part.Phys.Proc. **260**, 155-159 (2015)
[18] P. Eckert, *PhD Thesis* (Heidelberg University, 2015)
[19] W. Shen et al., NSS/MIC **C10-10-30**, 406-408 (2010)
[20] T. Harion et al., JINST **9**, C02003 (2014)
[21] D. Wiedner et al., JINST **9**, C01011 (2014)
[22] S. Agostinelli et al., Nucl.Instrum.Meth. **A506**, 250-303 (2003)
[23] J. Allison et al., IEEE Trans.Nucl.Sci. **53**, 270 (2006)